Ab initio calculations of the spectral shapes of CO_2 isolated lines including non-Voigt effects and comparisons with experiments

J.-M. Hartmann,[1,*] H. Tran,[1] N. H. Ngo,[1] X. Landsheere,[1] P. Chelin,[1] Y. Lu,[2] A.-W. Liu,[2] S.-M. Hu,[2] L. Gianfrani,[3] G. Casa,[3] A. Castrillo,[3] M. Lepère,[4] Q. Delière,[4] M. Dhyne,[4] and L. Fissiaux[4]

[1]*Laboratoire Interuniversitaire des Systèmes Atmosphériques (LISA) CNRS UMR 7583, Universités Paris Est Créteil et Paris Diderot, Institut Pierre-Simon Laplace, Université Paris Est Créteil, 94010 Créteil Cedex, France*

[2]*Hefei National Laboratory for Sciences at Microscale, University of Science and Technology of China, 230026 Hefei, China*

[3]*Dipartimento di Matematica e Fisica, Seconda Università di Napoli, Via Vivaldi 43, I-81100 Caserta, Italy*

[4]*Laboratoire Lasers et Spectroscopies, Research Centre in Physics of Matter and Radiation (PMR), University of Namur (FUNDP), 61 rue de Bruxelles, B-5000 Namur, Belgium*

(Received 8 October 2012; published 2 January 2013)

We present a fully *ab initio* model and calculations of the spectral shapes of absorption lines in a pure molecular gas under conditions where the influences of collisions and of the Doppler effect are significant. Predictions of the time dependence of dipole autocorrelation functions (DACFs) are made for pure CO_2 at room temperature using requantized classical molecular dynamics simulations. These are carried, free of *any* adjusted parameter, on the basis of an accurate anisotropic intermolecular potential. The Fourier-Laplace transforms of these DACFs then yield calculated spectra which are analyzed, as some measured ones, through fits using Voigt line profiles. Comparisons between theory and various experiments not only show that the main line-shape parameters (Lorentz pressure-broadening coefficients) are accurately predicted, but that subtle observed non-Voigt features are also quantitatively reproduced by the model. These successes open *renewed* perspectives for the understanding of the mechanisms involved (translational-velocity and rotational-state changes and their dependences on the molecular speed) and the quantification of their respective contributions. The proposed model should also be of great help for the test of widely used empirical line-shape models and, if needed, the construction of more physically based ones.

DOI: 10.1103/PhysRevA.87.013403 PACS number(s): 33.70.Jg, 34.10.+x

I. INTRODUCTION

The shape of gas-phase absorption spectra is of interest in this paper because it carries signatures of intermolecular interactions [1] and thus enables a test of collisional models and intermolecular potentials. For collisionally isolated lines (i.e., no line-mixing effects; see Chap. IV of [1]), tunable lasers have early demonstrated the approximate nature of the Voigt profile (e.g., [2–4] and Chap. III of [1]). These studies have had many followers and non-Voigt effects are nowadays evidenced to an unprecedented degree of detail thanks to the huge signal-to-noise ratio of some experiments (e.g., [5–7]). As is well known, both the molecules' center-of-mass velocity changes (VC) [8,9] and the speed dependence (SD) of the changes of the rotational state (broadening and shifting coefficients) [10,11] induced by collisions contribute to the line profile. In order to describe these effects, a *plethora* of models has been proposed (see Table III.6 of [1]) in which VC and SD, and their eventual temporal correlations, are empirically described with parameters fitted to experiments (e.g., [5,12–15]). Such simple approaches remain very popular but many are based on oversimplified descriptions of both VC (hard [16] or soft [9] collisions) and SD (quadratic [17] or confluent hypergeometric [10] laws). More physically based models have been proposed in which information on VC and/or SD is obtained independently from molecular dynamics simulations and/or semiclassical or quantum calculations, respectively (e.g., [18–23]). They have enabled accurate line-shape modelings but still rely on adjustments of some quantities [22,23]. Finally, first-principle fully *ab initio* quantum approaches are available (see Sec. III.5 of [1]) but, due to their complexity and computational cost, very few practical applications have been made. In this respect, only diatomic molecules with large rotational constants colliding with atoms have been considered [24–26]. This brief review indicates that no tractable *ab initio* approach has been proposed for pure polyatomic gases. Finally, note that first-principle approaches provide *reference benchmarks* that can greatly help in answering two questions still unanswered for many molecular systems: Which physical processes are involved in the line shape and what are their relative contributions? What is the proper empirical line profile to be used for fits of measured spectra? Solving these issues would be satisfactory for our physical understanding but it would also have important practical implications for spectroscopic databases and calculations of atmospheric spectra [27–29].

This paper presents a fully *ab initio* model suitable (today) for calculations of the line shapes in (some) molecular gas mixtures. It is applied to CO_2, based on a refined intermolecular potential [30] without use of any adjusted parameter, and successfully compared with measurements from various sources. The remainder of this paper is divided into four sections. The theoretical model and its input data are the subject of Sec. II. The experimental spectra used and the procedure retained for the analyses of measured and calculated absorptions are described in Sec. III. The results are presented and discussed in Sec. IV before concluding remarks and paths for future studies in Sec. V.

*Corresponding author: jean-michel.hartmann@lisa.u-pec.fr

II. CALCULATION OF THE SPECTRAL SHAPE AND DATA USED

A. Absorption coefficient

As is well known [1], the normalized absorption coefficient resulting from the interaction of a molecule-intrinsic (i.e., *not* interaction-induced [31–33]) dipole with an electromagnetic field of angular frequency ω and wave vector $\vec{k} = (\omega/c)\vec{z}$ is given by

$$F(\omega) = \mathrm{Re}\left\{\frac{1}{2\pi}\int_{-\infty}^{+\infty}\Phi(\omega,t)e^{-i\omega t}dt\right\}, \quad (1)$$

where $\Phi(\omega,t)$ is the autocorrelation function of the dipole $\vec{d}(t)$:

$$\Phi(\omega,t) = \langle e^{-i\vec{k}(\omega)\cdot\vec{q}(t)}\vec{d}(t)\cdot\vec{d}(0)e^{+i\vec{k}(\omega)\cdot\vec{q}(0)}\rangle. \quad (2)$$

In Eq. (2), $\langle\ldots\rangle$ denotes an average over the molecular system, $\vec{q}(t)$ is the molecule position, and the exponential terms result from the Doppler effect associated with the translational motion. As explained below, the approach proposed and used here for the calculation of $\Phi(\omega,t)$ is based on requantized classical molecular dynamics simulations (rCMDS).

B. Classical molecular dynamics simulations

Classical molecular dynamics simulations (CMDS) have been carried out as done for other purposes in previous successful studies [32–37] of various CO_2-radiation interactions properties. Since details can be found in these references; only a brief summary is given below. A total number $N_T = N_M N_B$ of linear and rigid (see discussion in Sec. II E) CO_2 molecules is considered. For parallel-computer calculations, they are distributed in N_B independent boxes, each of these being treated by a core and containing N_M molecules with periodic boundary conditions. Each molecule m is characterized by its center-of-mass position $\vec{q}_m(t)$ and velocity $\dot{\vec{q}}_m(t)$, by a unit vector $\vec{u}_m(t)$ along the molecule axis and the rotational angular momentum $\vec{\omega}_m(t)$ [alternatively $\dot{\vec{u}}_m(t)$]. After proper initializations of $\vec{q}_m(0)$, $\dot{\vec{q}}_m(0)$, $\vec{u}_m(0)$, and $\vec{\omega}_m(0)$ (Boltzmann statistics for energies and random vectors orientations), their evolutions with time are obtained from the equations of classical dynamics. In other words, the force and torque applied to each molecule by its surrounding sisters (through a pairwise anisotropic intermolecular potential) are computed at each time step. They lead to incremental elementary changes of the translational velocity and rotational angular momentum; these then induce changes of the position and axis orientation of the molecule.

For a dipole vector carried by the molecular axis (as it is the case for the asymmetric stretching $\Sigma - \Sigma$ absorption bands of CO_2 considered here), the (normalized at $t = 0$) dipole autocorrelation function is straightforwardly obtained from the CMDS results and given by

$$\Phi^{\mathrm{CMDS}}(\omega,t) = \frac{1}{N_T}\sum_{m=1,N_T} e^{-i\vec{k}(\omega)\cdot[\vec{q}_m(t)-\vec{q}_m(0)]}[\vec{u}_m(t)\cdot\vec{u}_m(0)], \quad (3)$$

from which the spectrum can be computed using Eq. (1). Note that only positive times are computed and that some approximations have been made which are discussed in Sec. II E.

C. Requantization

Autocorrelation functions obtained from the classical approach described above do not show the transient features [of periodicity $\pi I/\hbar = 1/(4cB) = 21.3$ ps, where I is the moment of inertia and $B = 0.39\,\mathrm{cm}^{-1}$, the rotational constant] due to rotational revivals. Their Fourier-Laplace transforms [Eq. (1)] thus lead to continuous spectra [33,34] showing *no* line structure. A requantization is thus necessary for which we use here a procedure similar to that successfully applied for the modeling of laser-induced alignment [35,37]. Following [38], for a molecule of (classical) rotational angular momentum $\omega_m = ||\vec{\omega}_m||$ we find the integer J_m (even for CO_2) for which $\hbar J_m/I$ or $\hbar(J_m+1)/I$ is the closest to ω_m. These two choices correspond to matching the $P(J_m)$ or $R(J_m)$ line position, respectively. Once J_m is found, ω_m is requantized by applying the change $\omega_m = \hbar J_m/I$ or $\omega_m = \hbar(J_m+1)/I$ while keeping the orientation $\vec{\omega}_m/||\vec{\omega}_m||$ of the rotational angular momentum unchanged. As in [35], this is applied only when the torque due to intermolecular interactions is below a properly chosen value (in order to let rotational-speed changes build up during collisions). Note that while it is possible to discriminate between R and P lines by considering the direction in which the molecule rotates [38], we have chosen not to do so for simplicity. All molecules in a rCMDS run have thus been requantized according to a single (P or R) criterion, an approximation discussed in Sec. II E.

D. Data used and implementation

We have used a CO_2 molar mass of $M = 44$ g/mole, a C-O bond length of 1.16 Å, and retained the CO_2-CO_2 site-site anisotropic potential energy surface of [30]. As shown in [32,33,35–37,39–41], the latter leads to very satisfactory predictions of numerous CO_2 properties. Using these data, rCMDS have been made on the IBM Blue Gene/P computer of the Institut du Développement et des Ressources en Informatique Scientifique. $N_B = 4096$ cores were used, each treating $N_M = 4000$ molecules thus leading to $N_T \approx 16\times10^6$. As noted previously [33,34] and shown in Fig. 1, a large number N_T is required to conveniently sample the phase space and to obtain, from Eq. (3), a converged average with little residual "noise."

It is easy to show that, provided that collisions remain essentially binary,[1] calculations made for a pressure P and a radiation angular frequency ω lead, after division (respectively, multiplication) of the time (respectively, frequency) scale by β, to autocorrelation functions (respectively, spectra) identical to those obtained for $P' = \beta\times P$ and $\omega' = \beta\times\omega$. This property is interesting because results for various values of the Lorentz to Doppler broadenings ratio Γ_L/Γ_D can be obtained in a

[1]This approximation is valid at the pressures (<0.5 atm) considered in this paper since the average time interval between successive collisions (respectively, mean free path) is more than two orders of magnitude greater than the duration of efficient collisions (respectively, range of efficient interactions).

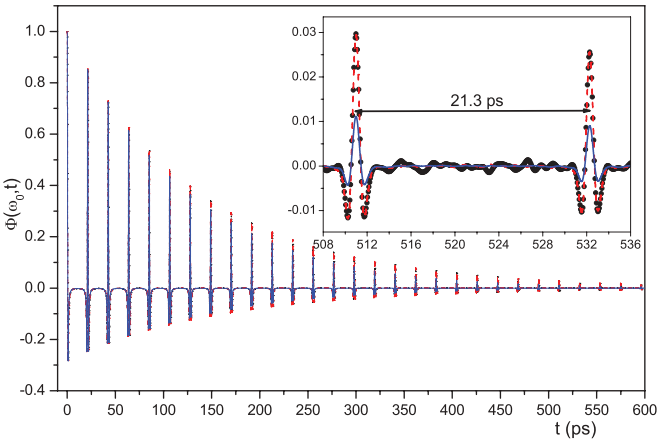

FIG. 1. (Color online) Normalized (at $t = 0$) calculated dipole autocorrelation functions (P lines) for 296 K and 0.4 bar with Doppler contributions corresponding to wave numbers of $\omega_0/2\pi c = 0$ (no Doppler, dashed red lines) and 20 000 cm^{-1} (solid blue line). The dotted black line and dashed red line in the inset have been obtained with no Doppler effect from calculations made with 1 and 16 million molecules, respectively.

single rCMDS run. Indeed, since absorption by a line centered at ω_0 is, at subatmospheric pressures, significant only in a very narrow frequency interval, one may safely replace $\vec{k}(\omega)$ by $\vec{k}(\omega_0)$ in Eq. (3). One can thus calculate, at each rCMDS time step, autocorrelation functions $\Phi(\omega_0,t)$ for several values of ω_0 at a negligible extra computer cost.

For the results presented in this paper, the temperature is 296 K and the pressure was set to 0.4 atm, a value offering a good compromise between the total time over which rCMDS must be carried [to ensure a large damping of $\Phi(\omega_0,t)$] and the spectral overlapping of adjacent lines (discussed in Sec. IV C). Twelve wave vectors (for the Doppler effect) corresponding to wave numbers [$\sigma_0 = \omega_0/2\pi c$] between 0 and about 2×10^5 cm^{-1} were used. With these choices the ratio Γ_L/Γ_D of the Lorentz to Doppler widths varies from infinity (collisional regime) down to about 0.2 (nearly Doppler regime). The rCMDS time step was set to $\delta t = 4$ fs, a value ensuring very small molecule displacements and rotations between successive times. Finally, calculations were carried up to $t_{\max} = 1300$ ps, a time delay for which the damping (of more than three orders of magnitude) of the autocorrelation functions is sufficient to make cutoff effects negligible while using Eq. (1).

E. Discussion of the approximations

Before discussing (and validating) the approximations made, let us emphasize that the proposed approach *intrinsically* takes into account almost all effects that condition the spectral shapes of the lines near their centers. Indeed, taken into account are uncompleted collisions and the finite collision duration; the translational velocities of the molecules (Doppler effect) and their changes induced by collisions (Dicke effect); the collision-induced changes of the rotational speeds of the molecules (collisional broadening) and their dependences on the initial molecular speed (speed dependence of the broadening); and the exchanges of population among the various rotational states (line mixing) and their dependences on the molecular translational speed (speed dependence of line mixing). The eventual temporal correlations between translational- and rotational-state changes due to collisions are obviously also taken into account.

Various approximations have been made in the approach described above, some being obvious while others are somehow hidden. They are discussed below where we try to evaluate their consequences on the quality of the predictions.

Classical CMDS. It is difficult to quantify the errors resulting from the requantized classical treatment of the CO_2 rotation. Nevertheless, due to the large moment of inertia of this molecule, one may believe that the errors are moderate, a statement reinforced by the quality of results obtained for other quantities [32,33,35,36].

Positive time calculation. The CMDS only calculate the evolution of the dipole autocorrelation function for positive times. To obtain the spectrum from Eq. (1) we thus assume $\Phi(\omega,-t) = \Phi(\omega,t > 0)$ which does not verify the relation [1] $\Phi(\omega,-t) = \Phi(\omega,t - i\hbar/k_BT)$. Hence, the spectra we calculate do not satisfy the fluctuation-dissipation theorem: $F(-\omega) = F(+\omega)e^{-\hbar\omega/k_BT}$. This is nevertheless of negligible importance if one considers the fact that, within the typical intervals of $\pm\Delta\sigma = 0.5$ cm^{-1} around a line center used in this work, $\exp(-\hbar\omega/k_BT)$ varies by less than 0.3% at 296 K.

Effects of vibration. All effects of vibrational motion have been disregarded in the rCMDS. In measured spectra, these manifest through the centering of the spectrum at the angular frequency ω_{Vib} with line profiles that depend on the considered absorption band through the dependence of the intermolecular potential on vibration. It is easy to correct calculated spectra for the first effect by simply shifting them by ω_{Vib}. On the other hand, the influence of the second effect cannot be taken into account easily. It results in vibrational shifts and broadenings of the spectral lines and can lead to an asymmetry of the profiles. These are discussed at the end of Sec. IV B where it is shown that their neglect does not significantly affect the quality of our predictions and the conclusions of this study.

Rigid-rotor assumption. This approximation neglects the centrifugal distortion and its consequences on the intermolecular potential and line positions. The first is obviously valid (and used in all collision models) since the relative elongation of the molecules is fully negligible for the rotational states populated at room temperature. The second effect is that the line positions obtained within the rigid-rotor model are wrong but without any consequences on the line shapes which are the subject of this paper.

Real dipole-vector autocorrelation. The scalar product $\vec{u}_m(t) \cdot \vec{u}_m(0)$ in Eq. (3) is a purely real quantity while, in reality, $\vec{d}(t) \cdot \vec{d}(0)$ in Eq. (2) is complex valued. This difference arises, aside from the quantum effects discussed above, from the fact that we have disregarded the direction in which molecules rotate and any dephasing of the dipole due to collisions. As mentioned in Sec. II B, the first problem could be solved but it is of no consequence for the present study since it only affects the positions of the transitions. The second process is the dephasing of the dipole associated with the fact that the effects of intermolecular interactions for molecules in the lower and upper states of the optical transitions are different. In

the spectral domain this manifests by the well known pressure shifting of the transitions. Besides an overall displacement of the line which is of no consequence on the line shape itself, the collisional shifting induces an asymmetry of the absorption profile through its dependence on the molecules' speeds. This effect is further discussed in Sec. IV C.

Single-branch calculation. As explained in Sec. II C the requantization is based on a single (P or R line) criterion. As a result, for a P branch requantization, for instance, the calculated R branch spectrum is the exact symmetric of the P branch. While the erroneous line positions do not affect the study of individual line shapes, the main problem is that, since we have disregarded the direction in which molecules rotate, the line-mixing process is badly taken into account. Interbranch mixings, associated with transfers of population between $P(J)$ and $R(J')$ states are likely significantly overestimated and the intrabranch ones $[P(J)$–$P(J')]$ are thus underestimated. Indeed, within our approach, the coupling between the $P(J)$ and $R(J')$ lines is identical to that between the $P(J)$ and $P(J')$ transitions, a rough approximation since it is much easier [42] to change a molecule rotational angular momentum from $|\omega_J|$ to $|\omega_{J'}|$ (same rotation direction) that to $-|\omega_{J'}|$ (change of rotation direction). The local effects of line mixing near line centers are thus likely underestimated, nevertheless by a factor of 2 at the most, but tests (see Sec. IV C) show that they can be neglected for the $P < 0.5$ atm conditions of the present study.

III. EXPERIMENTAL DATA AND SPECTRA ANALYSIS METHOD

A. Experimental data

Deviations from the Voigt profile have been evidenced for many molecules and lines in numerous experimental studies. When restricted to pure CO_2 and laser absorption measurements (their limited spectral resolution and signal-to-noise ratio make Fourier-transform spectrometers little adapted for detailed line-shape analyses), nonexhaustive examples can be found in [14,43–49]. The number of available measured spectra is thus considerable, the extensive analysis of which is beyond the scope of the present paper. The latter aims at a conclusive test of the proposed model but more exhaustive comparisons between theory and experiments will be the subject of future studies. We have retained available spectra from [14,47,49,50] but restricted our study to the transitions listed in Table I, choices made for five reasons: (i) Using four different experimental sources enables intercomparisons and thus reliable conclusions if the results are consistent. (ii) The selected experiments altogether cover, with intervals in common, a wide range of values of the ratio Γ_L/Γ_D of the Lorentz to Doppler widths. They thus sample all regimes from the nearly Doppler one ($\Gamma_L/\Gamma_D \ll 1$) to the purely collisional one ($\Gamma_L/\Gamma_D \gg 1$). (iii) Very different spectral regions have been investigated, from 0.8 to 10 μm, with transitions involving a broad range of vibrational-quanta changes. This will enable us to test the assumption of the independence of the line profile on vibration. (iv) The retained transitions are negligibly contaminated by neighboring lines, which simplifies the analysis of their experimental profiles. (v) Finally, the rotational quantum numbers of these four transitions ($|m| = 13,14,15$, and 16) are close so that the non-Voigt effects on their spectral shapes are expected to be nearly identical. Note that all spectra were recorded with lasers most of which have emission widths (<1 MHz) narrow enough to neglect the instrumental function. When not the case, the influence of this function has been taken into account in the spectra fits [47].

In addition to these experimental spectra, values of the broadening coefficients obtained for many lines from Voigt fits of Fourier-transform spectra have also been used. The data of [51] have been retained, which are in good agreement with previous measurements [52,53] and the ones of the present study. From analysis of the differences between the results in the two bands studied in [51] an uncertainty of ±2% was retained.

B. Spectra analysis method

For the analysis of both the calculated and measured absorption spectra and the test of the proposed model, we have used an approach similar to that of [22,23,54]. For each transition and pressure, the absorption coefficient $\alpha(\sigma)$ versus wave number ($\sigma = \omega/2\pi c$) is fitted, over an interval including the line center and near wings, by using a Voigt profile and a linear baseline. The Doppler width Γ_D is *fixed* to its theoretical value for the considered temperature while the line-center position σ_0, integrated intensity S (area), and Lorentz width Γ_L are floated together with the a and b parameters of the $a\sigma + b$ baseline. For the analysis of the results, we have retained four quantities: (1) and (2) When carried for various pressures P, the fits provide a set of collisional-broadening coefficients $\gamma_L(P) = \Gamma_L/P$. The asymptotic value in the collisional regime ($\Gamma_L/\Gamma_D \gg 1$) is a first quantity for comparison between measurements and calculations. Furthermore, the dependence of $\gamma_L(P)$ on pressure, if not constant, is a first signature on non-Voigt effects used for the test of the model. (3) We also retained the fit residuals normalized by the absorption peak value, i.e., $[\alpha^{\text{Expt or Calc}}(\sigma) - \alpha^{\text{Fit}}(\sigma)]/\alpha^{\text{Expt or Calc}}(\sigma_0)$. As is well known (e.g., [14,45,47–49]) and as shown by Figs. 2–4,

TABLE I. Spectra retained for the present study.

Line	σ_0 (cm^{-1})	$10^3\Gamma_D$ (cm^{-1})	Band	P range (mb)	Number of spectra	Γ_L/Γ_D range	Reference
$P(16)$	12758.48	11.89	$\nu_1 + 5\nu_3$	66–395	20	0.56–3.32	Ref. [49]
$P(14)$	12760.95	11.89	$\nu_1 + 5\nu_3$	66–395	13	0.56–3.32	Ref. [49]
$R(12)$	6237.42	5.79	$3\nu_1 + \nu_3$	20–620	22	0.35–10.7	Ref. [50]
$R(12)$	4948.62	4.60	$\nu_1 + 2\nu_2 + \nu_3$	6–40	30	0.14–0.87	Ref. [14]
$R(14)$	971.93	0.90	$\nu_3 - \nu_1$	29–66	4	3.21–7.30	Ref. [47]

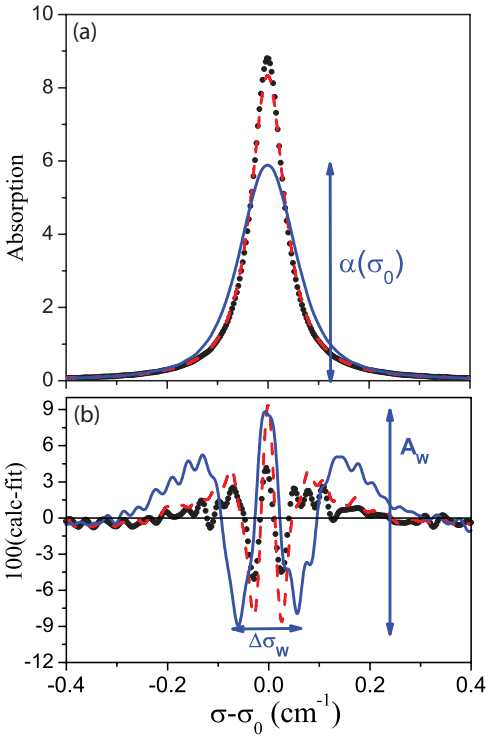

FIG. 2. (Color online) (a) Calculated area-normalized spectra for the $P(20)$ line at 0.4 bar and 296 K ($\Gamma_L \approx 0.04$ cm^{-1}) and Doppler widths Γ_D for which $\Gamma_L/\Gamma_D = 8.6$ (black dots), 2.5 (dashed red line), and 0.75 (blue line). The residuals of their fits with Voigt profiles, multiplied by 100, are displayed in(b).

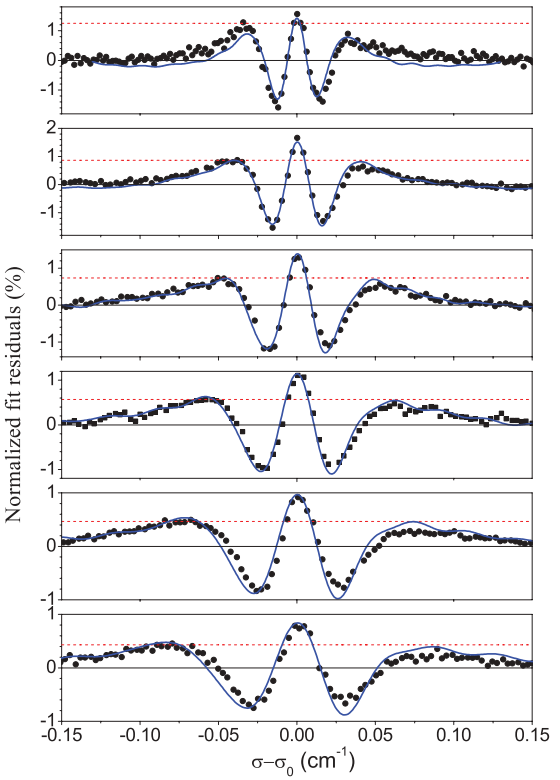

FIG. 3. (Color online) Voigt-fit residuals normalized by the absorption peak values for the $P(14)$ line at pressures from 50 Torr (top) to 300 Torr (bottom); (step 50 Torr). The (black) symbols are obtained from measured spectra [49] in the $\nu_1 + 5\nu_3$ band while the (blue) lines result from fits of rCMDS calculated spectra. The dashed red line matches the first maximum in the fit residuals of measured spectra to indicate the left-right asymmetry.

these residuals have a "W" shape characteristic of a line narrowing. The (max-min) amplitude of this W [indicated as $A_W/\alpha(\sigma_0)$ in Fig. 2] is a second non-Voigt signature for quantitative comparisons between theory and experiments. (4) Since we now have the width of the Voigt profile (through Γ_L and Γ_D) and the amplitude of the residuals [through $A_W/\alpha(\sigma_0)$] an additional parameter needed to characterize the line shape is the spectral extent of the residuals. For its "measure," we have retained the spectral distance between the two minima of the residuals (indicated as $\Delta\sigma_W$ in Fig. 2). At this step we have not considered the eventual asymmetry of the line shape, but this issue is discussed at the end of Sec. IV B.

IV. RESULTS AND DISCUSSION

A. Theoretical predictions

Typical dipole autocorrelation functions calculated at 0.4 bar and 296 K from Eq. (3) are plotted in Fig. 1, calling for several "positive" remarks. The first is that, thanks to requantization, rotational revivals are obtained with the proper period of $\pi I/\hbar = 21.3$ ps. The second is that, without the Doppler effect (dashed red line), the amplitudes of the revivals decrease quasiexponentially with a time constant $\tau \approx 148$ ps that does correspond, in the wave-number domain, to a value $\gamma = 1/(2\pi c\tau P) \approx 0.091$ cm^{-1}/atm close to the average self-broadening coefficient of CO_2 lines (see Fig. 5). When introducing Doppler effects, an additional damping is observed which is close to the Gaussian function expected from the Doppler contribution to the autocorrelation function. Furthermore, rCMDS made at very low pressure (10^{-9} bar) have led to a spectrum with almost perfectly Gaussian lines whose fits gave Doppler widths Γ_D agreeing within 0.1% with the theoretical ones, another successful test of our calculations. Finally, the comparison of the dotted black and dashed red lines in the insert, obtained for the same conditions but with 1 and 16 million molecules, respectively, demonstrates the need to treat many molecules in order to reduce the "noise" due to not fully converged statistics.

Examples of calculated spectra are plotted in Fig. 6 where results of independent computations for the P and R branches have been juxtaposed. As it should be, the lines have the positions of $-2BJ$ and $2B(J+1)$ in the P and R branches, respectively, which is expected from the rigid-rotor approximation. Furthermore, the intensities do reproduce the populations of the initial levels of the transitions since the dipole transition moment is assumed independent of the rotational state. In spectroscopic terms, this means that Herman Wallis corrections are neglected and that the Hönl-London factor is assumed equal to $J + \frac{1}{2}$. This is of no consequence for the line-shape study since it only affects the integrated intensities (areas) of the lines.

Typical fits of calculated spectra with Voigt profiles are displayed in Fig. 2 for various values of the Doppler width Γ_D relative to the collisional one Γ_L. As can be seen, W-shaped residuals are obtained, as experimentally observed (e.g.,

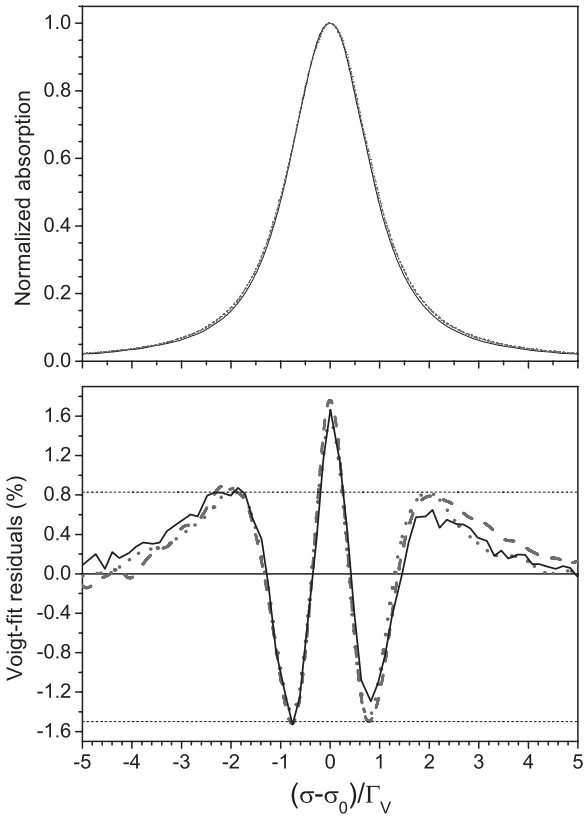

FIG. 4. Spectra (normalized to the peak value) and Voigt-fit residuals normalized by the absorption peak for a Γ_L/Γ_D ratio of 1.10. The results obtained from measured spectra are for the $P(14)$ line at 12 760.95 cm^{-1} for a pressure of 100 Torr [49] (black line) and for the $R(12)$ line at 12 760.95 cm^{-1} and a pressure of 49 Torr [50] (dashed red line). Also plotted are results obtained from rCMDS calculated spectra for the $P(14)$ line at the same value of Γ_L/Γ_D (dotted blue line).

[14,45,47–49] and Figs. 3 and 4). Furthermore, the amplitude of this W relative to peak absorption increases with decreasing Γ_L/Γ_D (for the studied range), a result also consistent with

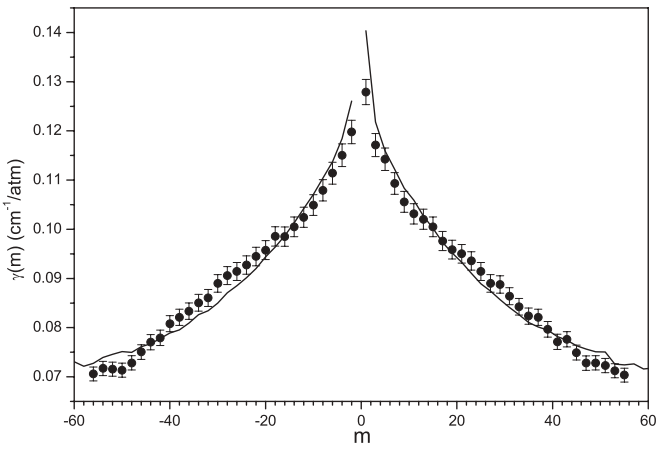

FIG. 5. (Color online) Pressure-normalized Lorentz broadening coefficients versus the rotational quantum number m ($= -J$ for P lines and $J + 1$ for R lines). The lines are results obtained from fit of the rCMDS calculated spectra without inclusion of the Doppler effect. The symbols are measured values [51] with error bars of ±2%.

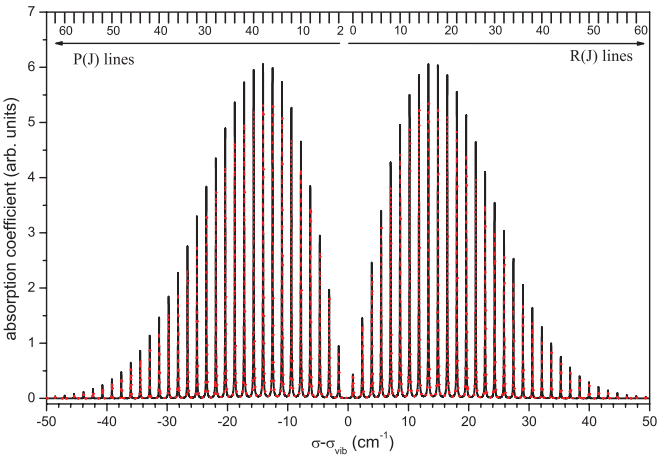

FIG. 6. (Color online) Calculated absorption spectra for 296 K and 0.4 bar with Doppler contributions corresponding to ratios of the collisional to Doppler widths of 13 (solid black line) and 1.7 (dotted red line). The lower-state rotational quantum numbers J of the lines are indicated on the top axis.

previous observations [22,23,54]. These predicted two non-Voigt signatures are quantitatively confirmed by experimental results in the next section. Note that the "noise" on the residuals (and spectra), would be reduced by using a larger number of molecules (see inset in Fig. 1) but could also be partly filtered out by fast Fourier transform (FFT) analysis.

B. Comparisons with experiments

Some of the spectra at our disposal result from repeated experiments and were recorded for the same (P, T, transition) conditions. Rather than averaging them or the results of their fits, we have decided to present, in Figs. 7–9, all individual results in order to give a "taste" of the measurements' uncertainties. Similarly, the raw rCMDS calculated spectra have been used without any attempt to reduce (through FFT filtering, for instance) the noise due to the limited number of molecules treated. The predictions thus show some localized "bumps" that have no physical meaning but remain small enough not to affect the conclusions.

Values of the pressure-normalized line-broadening coefficients deduced from Voigt fits of the P and R branches' calculated spectra in the collisional regime (no Doppler) are compared to experimental determinations [51] in Fig. 5. Except for the $R(1)$ and $P(2)$ transitions, our predictions are in good agreement with measured values with relative differences generally smaller than 2% and 4% at the most, quite a success for calculations free of any adjusted parameter. Discrepancies may be partly due to the intermolecular potential used [30], an issue which will be investigated in the future using the potentials of [55] and [56]. The bumps in the theoretical results for large $|m|$ result from the noise in the calculated absorptions for these relatively weak (see Fig. 6) transitions.

Voigt-fit retrieved broadening coefficients γ_L are plotted in Fig. 7 versus Γ_L/Γ_D. In order to carry comparisons between results obtained for different lines, the results have been normalized, for each transition, by the corresponding broadening coefficient γ_{Ref} given in [51]. A first comment is that the present experimental determinations are in good agreement

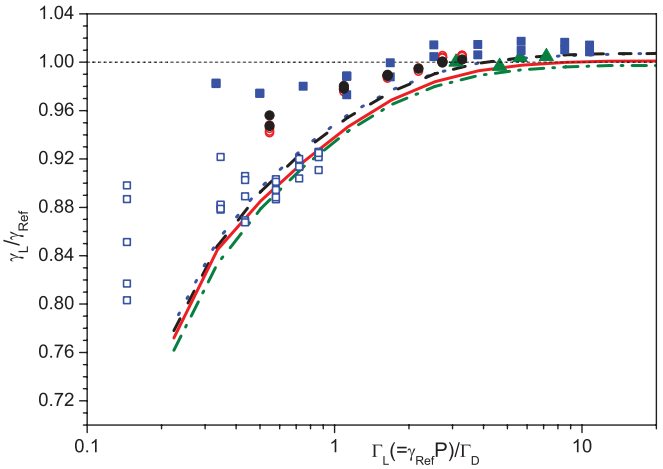

FIG. 7. (Color online) Observed (symbols) and calculated (lines) collisional-broadening coefficient per unit pressure $\gamma_L = \Gamma_L/P$ normalized by the value γ_{Ref} given in [51]. The results are plotted versus the ratio of the typical collisional-broadening coefficient $\Gamma_L = \gamma_{\text{Ref}} \times \text{P cm}^{-1}$ HWMH to the Doppler HWMH. The results are for the $P(16)$ (red open circles and red line), $P(14)$ (black solid circles and dashed black line), $R(12)$ (open and solid blue squares and dotted blue line), and $R(14)$ (olive triangles and dash-dotted olive line) transitions. The experimental results are from fits of the spectra of Refs. [48] [$P(16)$ and $P(14)$], [14] [$R(12)$], [47] [R(14)], and [50] [R(12)].

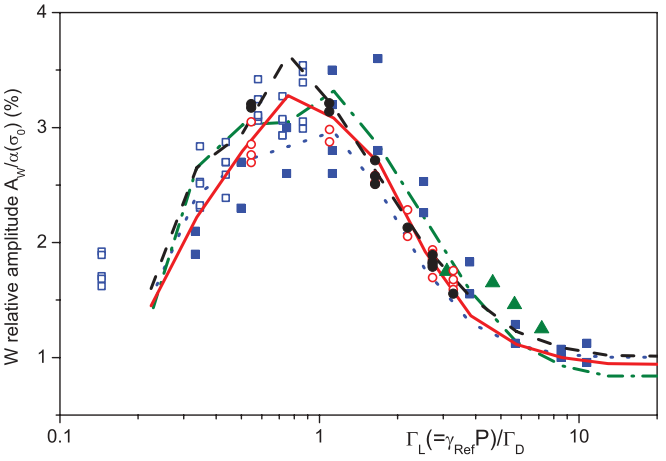

FIG. 8. (Color online) Same as Fig. 7 but displaying the relative amplitude $A_W/\alpha(\sigma_0)$ (see Fig. 2) of the W-shaped Voigt-fit residuals.

with each other. Furthermore, they are all consistent, in the high Γ_L/Γ_D limit, with the values of [51], as shown by the fact that the "eye-made" asymptotic values are within the [1.00,1.02] interval. As expected from Fig. 5 this statement also applies to the calculated results. Note that Fig. 7 also validates (within uncertainties) the assumption of the negligible effects of vibration on the line widths. Indeed, for the lines ($|m| \approx 15$) and vibrational bands studied here, differences in $\gamma_L(+\infty)$ remain below the 1%–2% uncertainty, a finding consistent with the predictions of [57]. The second point is that predictions satisfactorily reproduce the dependence of the broadening coefficient on Γ_L/Γ_D, a proof of the ability of the model to describe non-Voigt effects. It nevertheless seems that calculations may overestimate the decrease of γ_L with decreasing Γ_L/Γ_D, a result for which we have no definitive explanation at this point. A possible theoretical reason that will be explored in the near future is the intermolecular potential used. An alternative (complementary) explanation is experimental uncertainties. Indeed, for $\Gamma_L/\Gamma_D \ll 1$ the line shape is nearly the Gaussian Doppler one and the contribution of Γ_L to the spectrum becomes very small. Indeed, simulations made with a Voigt profile show that for $\Gamma_L/\Gamma_D = 1$, a change of 10% of Γ_L locally changes the absorption by only 0.2% of the peak value while the half width at half maximum (HWHM) of the profile changes by 0.5%. The experimental determination of Γ_L at very low pressures may thus be significantly uncertain as confirmed by the scatter of measured values for $\Gamma_L/\Gamma_D < 0.5$ in Fig. 7. Very careful high-quality experiments repeated for the same conditions would likely help in clarifying this issue. Finally note that dependences similar to those in Fig. 7 have been observed previously (e.g., [5,22,54,58–61]) and that the results are explained by the fact that the Voigt fits "do their best" to take the line narrowing into account.

The quality of the model is confirmed by the Voigt-fit residuals' relative amplitudes $A_W/\alpha(\sigma_0)$ (see Fig. 2) plotted in Fig. 8, since both their magnitudes and dependences on Γ_L/Γ_D are accurately predicted. While our Fig. 8 is for CO_2, similar results have been obtained for H_2O [22,54]. The main features are an asymptotic value in the collisional regime for $\Gamma_L/\Gamma_D \gg 1$ and a maximum around $\Gamma_L/\Gamma_D \approx 1$ followed by a decrease when going toward the Doppler regime for $\Gamma_L/\Gamma_D \ll 1$. This behavior can be easily explained. Indeed, as long as $\Gamma_L/\Gamma_D \gg 1$ the spectral shape does not depend on Γ_L/Γ_D if the wave-number scale is normalized by Γ_L (or pressure) [54] and the narrowing signature, purely due to the speed dependence, is independent of Γ_L/Γ_D. Then, with the increasing participation of the Doppler (and Dicke) effect, the narrowing increases to reach a maximum before residuals tend to zero when collisional effects become more and more negligible and the line shape becomes essentially Gaussian.

The last quantity retained for overall comparisons of measurements and calculations is the "width" $\Delta\sigma_W$ (see Fig. 2) of the residuals. In order to compare all data, one must normalize this quantity. For this, the line width (HWMH) Γ_V of the Voigt profile for the considered measurement or calculation conditions is a natural candidate. For its calculation, we have used the following expression [62]:

$$\Gamma_V = 0.5346 \times \Gamma_L + \sqrt{0.2166 \times \Gamma_L^2 + \Gamma_D^2}. \qquad (4)$$

The results, plotted in Fig. 9, give a final confirmation of the robustness of the proposed model. Note that the main panel in Fig. 9 may be misleading since the normalization by the Voigt width Γ_V masks large variations of $\Delta\sigma_W$, as shown by the inset. One can see that the values do show the expected asymptotic behaviors at low pressure (where $\Delta\sigma_W$ tends to be constant since the line shape becomes independent on pressure) and high pressure (where $\Delta\sigma_W$ increases linearly together with the width of the line). The limit $\Delta\sigma_W/2 \rightarrow \Gamma_D$ for $\Gamma_L/\Gamma_D \rightarrow 0$ is easy to understand since the profile then tends to its asymptotic Doppler limit with a HWHM of Γ_D. On the other hand, $\Delta\sigma_W/2 \rightarrow \approx 0.7\Gamma_L$ when $\Gamma_L/\Gamma_D \rightarrow$

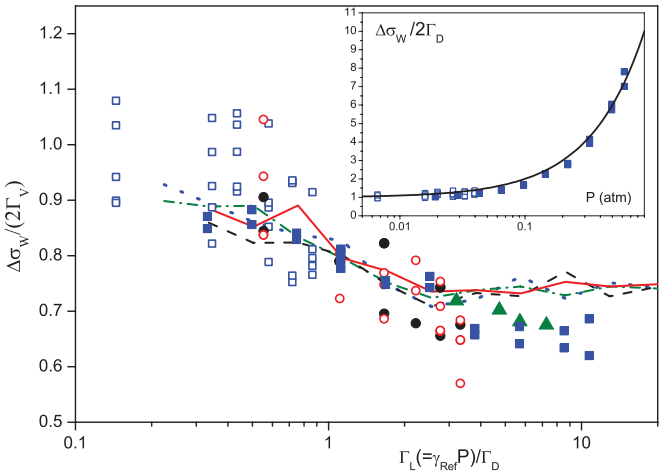

FIG. 9. (Color online) Same as Fig. 7 but displaying the "width" $\Delta\sigma_W$ (see Fig. 2) of the W-shaped Voigt-fit residuals normalized by the Voigt width [Eq. (4)]. The inset presents, versus pressure, the values of $\Delta\sigma_W$ normalized by the full Doppler width (FWHM) and obtained from the $R(12)$ line measurements of [14] (open squares) and [50] (solid squares) and the empirical linear fit $\Delta\sigma_W/2\Gamma_D = 1 + 10 \times P(\text{atm})$ (line).

$+\infty$ is an experimental (and theoretical) result whose analysis remains to be made.

An issue not discussed up to now is the eventual asymmetry of the line shapes near the line centers, to which four processes may participate [1], which are the contributions of the wings of the surrounding transitions, the finite duration of collisions, line mixing, and the speed dependence of the pressure shifting coefficients. The first three mechanisms, present in both calculated and measured spectra, are discussed in the next section where it is shown that they can be neglected for the $P < 0.5$ atm, 296 K conditions considered in this study. The situation for the shift is different since, as discussed in Sec. II E, the rCMDS do not take into account the dephasing of the dipole and, consequently, the calculated spectra cannot show any shift-induced asymmetry. This may introduce a bias in the comparisons in Figs. 7–9, an issue that we now discuss. Recall that the pressure-induced shifting coefficients δ_L strongly increase with the number of vibrational quanta of the optical transition [63], in opposition to the pressure broadening whose vibrational dependence is negligible [57]. For pure CO_2 at room temperature and the considered lines of the $\nu_3 - \nu_1$, $\nu_1 + 2\nu_2 + \nu_3$, $3\nu_1 + \nu_3$, and $\nu_1 + 5\nu_3$ bands, the experimentally determined values of δ_L are -0.0032 cm^{-1}/atm [64], -0.0051 cm^{-1}/atm [52], -0.0053 cm^{-1}/atm [51,52], and -0.0135 cm^{-1}/atm [49], respectively. These shifts manifest in the spectrum through displacements of the line centers which are not relevant for the present line-shape study and are taken into account through the adjustment (see Sec. III B) of the line position σ_0. They also induce, through their speed dependences, asymmetries of the line profiles with, δ_L being negative, enhancements of the low frequency of the line with respect to the high-frequency one (e.g., [13,65–67]). The relative asymmetry is obviously all the greater as the ratio δ_L/γ_L of the shifting to broadening is large, as confirmed by [13,67]. From the numbers given above and the typical value (see Fig. 5) $\gamma_L \approx 0.1$ cm^{-1}/atm, δ_L/γ_L is below 6% except for the highest overtone lines considered here for which $\delta_L/\gamma_L \approx 14\%$. One thus expects asymmetries to be very small for transitions of the three first bands studied in this paper. In fact, the Voigt fits that we have made indicate that their spectral shapes are symmetric within noise and uncertainties, a result also shown in [47] ($\nu_3 - \nu_1$), [14,45] ($\nu_1 + 2\nu_2 + \nu_3$), and [43,44] ($3\nu_1 + \nu_3$). In order to go further, we now focus on the $P(14)$ transition of the $\nu_1 + 5\nu_3$ band at 12 760.95 cm^{-1} for which measurements have been made [49] at six pressures from 50 to 300 Torr. Dedicated rCMDS were carried out under exactly the same conditions and experimental and calculated spectra were fitted with Voigt profiles. The results, plotted in Fig. 3, confirm a slight asymmetry of measured profiles while the calculated ones (filtered by a low-pass FFT to reduce the oscillations observed in Fig. 2) are symmetric, as expected. The asymmetry of the measured profiles is small since differences between the observed residuals and the symmetrized ones remain, at the low- and high-frequency maxima and minima, lower than about $\pm 10\%$ (the full asymmetry thus being of $\sim 20\%$). Note that good agreement between measured and calculated results would be obtained if the former were symmetrized (using the average of the low- and high-frequency sides, for instance). These statements and the negligible asymmetry for lower overtones are confirmed by Fig. 4 where the wave-number scale has been normalized by the Voigt HWHM [Eq. (4)] in order to be able to compare the various results.

C. Mechanisms involved

As is well known, line mixing and finite collision-duration effects, in addition to velocity changes and speed dependence, are mechanisms which may affect the spectral shape. They can thus contribute to the residuals of Voigt fits of both calculated and measured spectra discussed above, together with the fact that the contributions of surrounding lines are only approximately modeled by the adjusted baseline. The following analysis tries to quantify the influences of these effects on the Voigt-fit results of the preceding section, in order to clarify the main mechanisms governing the spectral shape.

The collision duration for pure CO_2 at 296 K is typically a couple of picoseconds. It thus manifests, in the frequency domain, several tens of wave numbers away from the line centers. The resulting asymmetry is thus observable at elevated densities [68] but its consequences within the line core at lower pressures are negligible as confirmed in [12,69,70]. Furthermore, the small contribution that this effect may make to our experimental and calculated spectra is likely significantly reduced by the adjustment of a linear baseline.

For the quantification of the effects of neighboring lines and of line mixing, we have used the model of [71] whose quality is demonstrated in this reference. Full $\Sigma - \Sigma$ band spectra have first been calculated at different pressures by summing the various line contributions with Voigt profiles. Individual lines have then been adjusted, as explained in Sec. III B, yielding the associated fit residuals. The results show that, in the pressure range investigated in this study, the fact that the baseline only approximately takes neighboring lines' contributions into account leads to negligible residuals.

Indeed, relative to peak absorption, the latter remain below 0.02%, much smaller that the values in Fig. 8. A similar exercise was carried out starting from spectra calculated taking line mixing into account. The resulting fit residuals due to line mixing are about three times larger (0.06%) but still negligible when compared to the 1%–4% scale of Fig. 8.

The negligible influence of the effects discussed above is confirmed by both experimental and rCMDS calculated spectra. Indeed, all three lead to asymmetries of the line profile that, if significant, would translate in the Voigt-fit residuals. The fact that the signatures in Figs. 2 and 4 [for the $R(12)$ line] and in [14,45,47], for instance, are symmetric (within uncertainties) is a further demonstration that the results are not biased. Now that we have shown that the finite duration of collisions and line mixing have negligible influence, the line shape can be modeled using a simplified kinetic equation. Indeed, the latter may thus be written for the dipole autocorrelation function of a single transition within the impact approximation as done in [16,22,72–74], for instance. This greatly simplifies the problem since the "only" ingredients needed as inputs to this equation are descriptions of the speed-dependent rates for translational (velocity) and rotational (broadening and shifting) changes. The route is then opened for the test of simple modeling of these processes as discussed below.

V. CONCLUSION AND PERSPECTIVES

This paper presents a model for the *ab initio* calculation of individual line shapes *directly* from the intermolecular potential and without use of *any* adjusted parameter. Comparisons between measured and calculated results for pure CO_2 demonstrate that this approach very satisfactorily reproduces the pressure broadening and the non-Voigt effects. In spite of this success, the quality of the predictions cannot, in our opinion, compete with the precision of modern laser experiments. Our model and its results are nevertheless a major step toward solving, for CO_2, the still unanswered questions: What are the physical processes involved in the line shape and what are their relative contributions? What is the proper empirical line profile to be used for fits of measured spectra? The rCMDS, as carried out in this work, are useless for this purpose since they are some kind of "black box" that directly provides the spectrum. Nevertheless, a solution could be brought through a five-step strategy as follows: (1) Extract, from exactly the *same* rCMDS, information on the evolutions with time of the molecules' velocities and rotational states. From these one can deduce data on translational (e.g., [20]) and rotational (e.g., [34]) changes and their correlation (e.g., [22]) as well as on the speed dependence of the broadening coefficients. (2) Use these data to test available simple models for velocity changes (VC) [9,16,75,76] and speed dependences (SD) [10,17], as done for VC in [20], for instance. (3) If necessary, construct alternative empirical approaches for better descriptions of the rCMDS-predicted VC and SD. (4) Combine the retained simple VC and SD models into a kinetic equation for the dipole autocorrelation function in order to compute the spectrum, as done in [20,22,66] and check the quality of the resulting predictions by direct comparisons with the rCMDS-calculated spectra. If there is good agreement, the second question mentioned above will have found an answer. (5) The kinetic equation and its inputs describing VC, SD, and the eventual temporal correlation between translational and rotational changes can then be used to analyze the respective contributions to the line shape. This can be easily done by turning on, turning off, or scaling the VC and/or SD and/or temporal correlation, bringing an answer to the first question. Such research will be the subject of our future studies in which extended treatments of experimental data and new measurements will be made for larger scale tests of theoretical approaches. This includes investigations for many lines, pressures, temperatures, and CO_2-X mixtures, while rCMDS will be carried with various intermolecular potential energy surfaces. Let us emphasize that the results in Figs. 7– 9 demonstrate the *importance* for future experimental studies to investigate, when possible, a pressure range for which the ratio Γ_L/Γ_D of the collisional to Doppler widths varies from $\ll 1$ to $\gg 1$. Measurements in limited ranges bring only partial information that may not enable reliable conclusions on the processes involved and on the quality of models.

Note that, while rCMDS have been proved to enable accurate predictions of numerous CO_2 spectral properties (this paper and [32,33,36,37]), this is due to the large moment of inertia of this molecule which makes a classical treatment of its rotation appropriate. It is thus not a general conclusion and rCMDS would likely give much less satisfactory results for molecules with large rotational constants for which the quantum nature of rotational states must be rigorously taken into account. Furthermore, the requantization procedure used, essential to calculate line spectra, is easy to implement for linear molecules, more complicated but feasible for symmetric-top molecules, but impossible for asymmetric-top molecules, a further limitation of the proposed model.

ACKNOWLEDGMENTS

The authors from LISA thank the Institut du Développement et des Ressources en Informatique Scientifique (IDRIS) for providing access to the IBM Blue Gene/P parallel computer. They also acknowledge financial support from the Terre, Océan, Surfaces Continentales, Atmosphère program of the Centre National d'Etudes Spatiales.

[1] J. M. Hartmann, C. Boulet, and D. Robert, *Collisional Effects on Molecular Spectra: Laboratory Experiments and Models, Consequences for Applications* (Elsevier, Amsterdam, 2008).
[2] J. Ritter and T. D. Wilkerson, J. Mol. Spectrosc. **121**, 1 (1987).
[3] A. S. Pine and J. P. Looney, J. Mol. Spectrosc. **122**, 41 (1987).
[4] B. E. Grossmann and E. V. Browell, J. Mol. Spectrosc. **139**, 562 (1989).
[5] D. A. Long, K. Bielska, D. Lisak, D. K. Havey, M. Okumura, C. E. Miller, and J. T. Hodges, J. Chem. Phys. **135**, 064308 (2011).

[6] M. D. De Vizia, A. Castrillo, E. Fasci, L. Moretti, F. Rohart, and L. Gianfrani, Phys. Rev. A **85**, 062512 (2012).
[7] A. Cygan, D. Lisak, S. Wójtewicz, J. Domysławska, J. T. Hodges, R. S. Trawiński, and R. Ciuryło, Phys. Rev. A **85**, 022508 (2012).
[8] R. H. Dicke, Phys. Rev. **89**, 472 (1953).
[9] L. Galatry, Phys. Rev. **122**, 1218 (1961).
[10] P. R. Berman, J. Quant. Spectrosc. Radiat. Transfer **12**, 1331 (1972).
[11] H. M. Pickett, J. Chem. Phys. **73**, 6090 (1980).
[12] A. S. Pine and R. Ciurylo, J. Mol. Spectrosc. **208**, 180 (2001).
[13] D. Lisak, J. Hodges, and R. Ciurylo, Phys. Rev. A **73**, 012507 (2006).
[14] G. Casa, R. Wehr, A. Castrillo, E. Fasci, and L. Gianfrani, J. Chem. Phys. **130**, 184306 (2009).
[15] M. D. De Vizia, F. Rohart, A. Castrillo, E. Fasci, L. Moretti, and L. Gianfrani, Phys. Rev. A **83**, 052506 (2011).
[16] S. G. Rautian and J. I. Sobel'man, Sov. Phys. Usp. **9**, 701 (1967).
[17] F. Rohart, H. Mäder, and H.-W. Nicolaisen, J. Chem. Phys. **101**, 6475 (1994).
[18] A. S. Pine, J. Quant. Spectrosc. Radiat. Transfer **62**, 397 (1999).
[19] P. Joubert, P. N. M. Hoang, L. Bonamy, and D. Robert, Phys. Rev. A **66**, 042508 (2002).
[20] H. Tran, J.-M. Hartmann, F. Chaussard, and M. Gupta, J. Chem. Phys. **131**, 154303 (2009).
[21] H. Tran, F. Thibault, and J.-M. Hartmann, J. Quant. Spectrosc. Radiat. Transfer **112**, 1035 (2011).
[22] N. H. Ngo, H. Tran, and R. R. Gamache, J. Chem. Phys. **136**, 154310 (2012).
[23] N. H. Ngo, H. Tran, R. R. Gamache, D. Bermejo, and J.-L. Domenech, J. Chem. Phys. **137**, 064302 (2012).
[24] R. Blackmore, S. Green, and L. Monchick, J. Chem. Phys. **91**, 3846 (1989).
[25] S. Green, R. Blackmore, and L. Monchick, J. Chem. Phys. **91**, 52 (1989).
[26] L. Demeio, S. Green, and L. Monchick, J. Chem. Phys. **102**, 9160 (1995).
[27] G. Durry, V. Zéninari, B. Parvitte, T. Le Barbu, F. Lefèvre, J. Ovarlez, and R. R. Gamache, J. Quant. Spectrosc. Radiat. Transfer **94**, 387 (2005).
[28] B. Barret, D. Hurtmans, M. R. Carleer, M. De Mazière, E. Mahieu, and P.-F. Coheur, J. Quant. Spectrosc. Radiat. Transfer **95**, 499 (2005).
[29] D. R. Thompson, D. C. Benner, L. R. Brown, D. Crisp, V. Malathy Devi, Y. Jiang, V. Natraj, F. Ovafuso, K. Sung, D. Wunch, R. Castano, and C. E. Miller, J. Quant. Spectrosc. Radiat. Transfer **113**, 2265 (2012).
[30] S. Bock, E. Bich, and E. Vogel, Chem. Phys. **257**, 147 (2000).
[31] L. Frommhold, *Collision Induced Absorption in Gases*, Cambridge Monographs on Atomic, Molecular, and Chemical Physics (Cambridge University Press, Cambridge, 2006).
[32] J.-M. Hartmann, C. Boulet, and D. Jacquemart, J. Chem. Phys. **134**, 094316 (2011).
[33] J.-M. Hartmann and C. Boulet, J. Chem. Phys. **134**, 184312 (2011).
[34] J.-M. Hartmann, C. Boulet, H. Tran, and M. T. Nguyen, J. Chem. Phys. **133**, 144313 (2010).
[35] J.-M. Hartmann and C. Boulet, J. Chem. Phys. **136**, 184302 (2012).
[36] J. Houzet, J. Gateau, E. Hertz, F. Billard, B. Lavorel, J.-M. Hartmann, C. Boulet, and O. Faucher, Phys. Rev. A **86**, 033419 (2012).
[37] T. Vieillard, F. Chaussard, F. Billard, D. Sugny, B. Lavorel, J.-M. Hartmann, C. Boulet, and O. Faucher, Phys. Rev. Lett. (submitted).
[38] R. G. Gordon, J. Chem. Phys. **45**, 1649 (1966).
[39] S. Bock, E. Bich, E. Vogel, A. S. Dickinson, and V. Vesovic, J. Chem. Phys. **117**, 2151 (2002).
[40] S. Bock, E. Bich, E. Vogel, A. S. Dickinson, and V. Vesovic, J. Chem. Phys. **120**, 7987 (2004).
[41] S. Bock, E. Bich, E. Vogel, A. S. Dickinson, and V. Vesovic, J. Chem. Phys. **121**, 4117 (2004).
[42] R. Rodrigues, C. Boulet, L. Bonamy, and J.-M. Hartmann, J. Chem. Phys. **109**, 3037 (1998).
[43] J. Henningsen and H. Simonsen, J. Mol. Spectrosc. **203**, 16 (2000).
[44] T. Hikida, K. M. T. Yamada, M. Fukabori, T. Aoki, and T. Watanabe, J. Mol. Spectrosc. **232**, 202 (2005).
[45] L. Joly, F. Gibert, B. Grouiez, A. Grossel, B. Parvitte, G. Durry, and V. Zéninari, J. Quant. Spectrosc. Radiat. Transfer **109**, 426 (2008).
[46] G. Casa, D. A. Parretta, A. Castrillo, R. Wehr, and L. Gianfrani, J. Chem. Phys. **127**, 084311 (2007).
[47] Q. Delière, L. Fissiaux, and M. Lepère, J. Mol. Spctrosc. **272**, 36 (2012).
[48] Y. Lu, A.-W. Liu, H. Pan, X.-F. Li, V. I. Perevalov, S. A. Tashkun, and S. M. Hu, J. Quant. Spectrosc. Radiat. Transfer **113**, 2197 (2012).
[49] Y. Lu, A.-W. Liu, X.-F. Li, J. Wang, C.-F. Cheng, Y. R. Sun, and S.-M. Hu (unpublished).
[50] Recordings of the $R(12)$ line of the $3\nu_1 + \nu_3$ band of pure CO_2 near 1.6 μm have been made at LISA using an apparatus similar to that of N. H. Ngo, N. Ibrahim, X. Landsheere, H. Tran, P. Chelin, M. Schwell, and J.-M. Hartmann, J. Quant. Spectrosc. Radiat. Transfer **113**, 870 (2012). These dedicated measurements will be extended to other lines and conditions with results presented, together with experimental details, in a forthcoming paper.
[51] A. Predoi-Cross, A. V. Unni, W. Liu, I. Schofield, C. Holladay, A. R. W. McKellar, and D. Hurtmans, J. Mol. Spectrosc. **245**, 34 (2007).
[52] R. A. Toth, L. R. Brown, C. E. Miller, V. Malathy Devi, and D. C. Benner, J. Mol. Spectrosc. **239**, 243 (2006).
[53] V. M. Devi, D. C. Benner, L. R. Brown, C. E. Miller, and R. A. Toth, J. Mol. Spectrosc. **242**, 90 (2007).
[54] H. Tran, D. Bermejo, J.-L. Domenech, P. Joubert, R. R. Gamache, and J.-M. Hartmann, J. Quant. Spectrosc. Radiat. Transfer **108**, 126 (2007).
[55] C. S. Murthy, S. F. O'Shea, and I. R. McDonald, Mol. Phys. **50**, 531 (1983).
[56] R. Bukowski, J. Sadlej, B. Jeziorski, P. Jankowski, K. Szalewicz, S. A. Kucharski, H. L. Williams, and B. M. Rice, J. Chem. Phys. **110**, 3785 (1999).
[57] R. R. Gamache and J. Lamouroux, J. Quant. Spectrosc. Radiat. Transf. (in press).
[58] B. E. Grossmann and E. V. Browell, J. Mol. Spectrosc. **136**, 264 (1989).
[59] B. E. Grossmann and E. V. Browell, J. Mol. Spectrosc. **138**, 562 (1989).

[60] P. L. Ponsardin and E. V. Browell, J. Mol. Spectrosc. **185**, 58 (1997).
[61] C. Claveau, A. Henry, M. Lepère, A. Valentin, and D. Hurtmans, J. Mol. Spectrosc. **212**, 171 (2002).
[62] J. J. Olivero and R. L. Longbothum, J. Quant. Spectrosc. Radiat. Transfer **17**, 233 (1977).
[63] J.-M. Hartmann, J. Quant. Spectrosc. Radiat. Transfer **110**, 2019 (2009).
[64] V. Malathy Devi, D. C. Benner, M. A. H. Smith, L. R. Brown, and M. Dulick, J. Quant. Spectrosc. Radiat. Transfer **76**, 411 (2003).
[65] D. Robert and L. Bonamy, Eur. Phys. J. D **2**, 245 (1998).
[66] L. Bonamy, H. Tran, P. Joubert, and D. Robert, Eur. Phys. J. D **31**, 459 (2004).
[67] B. E. Grossmann and E. V. Browell, J. Quant. Spectrosc. Radiat. Transfer **45**, 339 (1991)
[68] P. Marteau, C. Boulet, and D. Robert, J. Chem. Phys. **80**, 3632 (1984).
[69] C. Boulet, P.-M. Flaud, and J.-M. Hartmann, J. Chem. Phys. **120**, 11053 (2004).
[70] J. Boissoles, F. Thibault, C. Boulet, J.-P. Bouanich, and J.-M. Hartmann, J. Mol. Spectrosc. **198**, 257 (1999).
[71] H. Tran, C. Boulet, S. Stefani, M. Snels, and G. Piccioni, J. Quant. Spectrosc. Radiat. Transfer **112**, 925 (2011).
[72] D. A. Shapiro, R. Ciurylo, J. R. Drummond, and A. D. May, Phys. Rev. A **65**, 012501 (2001).
[73] D. A. Shapiro, R. Ciurylo, R. Jaworski, and A. D. May, Can. J. Phys. **79**, 1209 (2001).
[74] H. Tran and J.-M. Hartmann, J. Chem. Phys. **130**, 094301 (2009).
[75] J. Keilson and J. E. Storer, Quaterly Appl. Math. **10**, 243 (1952).
[76] M. J. Lindenfeld and B. Shizgal, Chem. Phys. **41**, 81 (1979).